DE GRUYTER Green Processing and Synthesis 2023; 12: 20230157

Research Article

Harshala Sandip Naik, Parvindar Manejar Sah, Manali Dhangade, Jaya Lakkakula, Rajesh Warluji Raut*, Arpita Roy*, Saad Alghamdi, Naeem Qusty, Zain Alhindi, Ahmed Kabrah, and Anju Rani

# Synthesis of a silica matrix with ZnO nanoparticles for the fabrication of a recyclable photodegradation system to eliminate methylene blue dye

https://doi.org/10.1515/gps-2023-0157
received August 22, 2023; accepted November 7, 2023

**Abstract:** In this study, a silica matrix was utilized as a substrate for zinc oxide nanoparticles (ZnO NPs) to enhance their photocatalytic activity for the degradation of methylene blue (MB) dye. The recovery of the prepared material was also investigated. To compare the performance of the prepared material with ZnO NPs and bare silica, various analyses were conducted. ZnO NPs were synthesized via a coprecipitation method and characterized using Fourier-transform infrared spectra and X-ray diffraction (XRD). The XRD results revealed highly crystalline ZnO NPs with an average crystallite size of less than 100 nm. The presence of ZnO on the silica matrix was confirmed using scanning electron microscopy (SEM) and EDX analysis. The prepared ZnO NPs showed enhanced photocatalytic activity for the degradation of MB dye, and reasonable material recovery was also observed. The silica-coated ZnO NPs degraded MB dye by 97% in just 40 min and retained their photocatalytic activity for up to 20 cycles. In comparison, bare silica exhibited effective photodegradation but lost its photodegradation capacity after five cycles. ZnO NPs without silica coating took 5 h to degrade MB dye. The significant accomplishment in this study is the development of novel materials with high recoverability, simple preparation, and efficient photocatalytic activity. In the future, ZnO NPs supported on a silica matrix can be utilized for various applications.

**Keywords:** silica matrix, ZnO nanoparticles, photocatalytic activity, recoverable matrix

## 1 Introduction

Dye is a significant colour category that finds use in the textile industry [1]. Methyl blue and methylene orange are commonly used as colouring agents [2]. The textile industry generates wastewater during various processes like bleaching, boiling, desizing, mercerizing, and printing [3]. The wastewater discharged from the dye industry contains chemicals, such as naphthalene, ammonia, chlorine, benzene, and anthraquinone, which cause damage to water bodies. Such colouring compounds affect photosynthesis and damage [4] the ecosystem [5]. Additionally, the dyes used in the textile industry are carcinogenic, toxic, and mutagenic, thereby posing a significant threat to human health [2]. Chlorine, commonly used in textile plants, can cause allergic reactions and skin irritation [2]. Therefore, it is imperative to manage wastewater discharged from textile industries suitably.

Removing dye from the environment poses a challenge for botanists, environmental scientists, and researchers. Several techniques, including membrane adsorption [6],

---

*** Corresponding author: Rajesh Warluji Raut,** Department of Botany, The Institute of Science, Dr. Homi Bhabha State University, 15, Madam Cama Road, Mumbai 400-032, India, e-mail: r_raut@rediffmail.com
*** Corresponding author: Arpita Roy,** Department of Biotechnology, Sharda School of Engineering & Technology, Sharda University, Greater Noida, India, e-mail: arbt2014@gmail.com
**Harshala Sandip Naik, Parvindar Manejar Sah:** Department of Botany, The Institute of Science, Dr. Homi Bhabha State University, 15, Madam Cama Road, Mumbai 400-032 India
**Manali Dhangade:** Department of Botany, The Institute of Science, Dr. Homi Bhabha State University, 15, Madam Cama Road, Mumbai 400-032, India
**Jaya Lakkakula:** Centre for Computational Biology and Translational Research, Amity Institute of Biotechnology, Amity University Maharashtra, Mumbai-Pune Expressway, Bhatan, Panvel, Mumbai, Maharashtra, 410206, India
**Saad Alghamdi, Naeem Qusty, Zain Alhindi, Ahmed Kabrah:** Department of Clinical Laboratory Sciences, Faculty of Applied Medical Sciences, Umm Al-Qura University, Makkah, Saudi Arabia
**Anju Rani:** Department of Life Sciences, Graphic Era Deemed to be University, Dehradun, Uttarakhand, India

advanced oxidation [7], electrochemical technique [8], and flocculation-coagulation [9], are available for the removal of dyes from environmental bodies. Among these techniques, adsorption using an adsorbent material is the most effective and cost-efficient method for treating wastewater from the dye industry [10]. The simplicity of this technique makes it an attractive option for wastewater treatment.

Currently, researchers are focusing on developing nanoparticles supported by an adsorbent material to enhance their adsorbent capacity, surface area, and degradation capacity. For instance, nanoparticles such as zinc [11–15], silver [16], gold [17], palladium [18], copper [19], nickel [20], magnesium [21], and titanium [22–24] have been utilized in the photodegradation of methylene blue (MB). During the dye degradation process, adsorbents like rice husk [25], orange peel [26], mango peel [27], coconut shell [28], chitosan [29], coffee bean [30], and banana peel [31] have been employed. However, a significant drawback of these adsorbents is that they cannot be separated or recovered from the reaction, and some inorganic adsorbents like natural silica [32], natural and synthetic nano clay [33], various types of sand [34], silica gel 60–120, silica gel 230–400, basic alumina, acidic alumina, alginate, and activated coffee [35] are utilized in the degradation of different dyes. A major disadvantage of these materials is that after a few cycles, they do not show recovery, and an external high temperature is required for recovery [35]. Therefore, a recovery process that does not require external temperature is necessary.

In most photodegradation studies using silica nanoparticles [32,36–39], silica decorated with nanoparticles like ZnO [40], $TiO_2$ [41], Cu–Ni [42], Fe–Co [43], $Fe_3O_4$–$SiO_2$–$CeO_2$ [44], and Ni–Zn [45], as well as attachment of biological functional groups such as cysteine [46] and folic acid [47] on silica are utilized as photocatalysts. Decorating silica with various compounds is a complicated process [22,25,42,44,46–48], and some require costly chemicals, in most cases, high-grade silica is used, which is expensive.

The photocatalytic degradation study of MB was conducted with silica, silica-coated zinc oxide (Silica@ZnO), and ZnO. The confirmation of degradation of MB was established by visual observation. After degradation, MB changes its colour from blue to colourless, indicating its degradation. The deep-blue colour of MB is due to its oxidizing state, and when reduced, it becomes colourless due to the formation of leuco MB. The peak observed initially after degradation becomes completely flat because of the formation of $CO_2$ and water [49].

In the present study, ZnO nanoparticles coated on silica mesh 60–120 were studied because it is a low-cost option. The normal coprecipitation method was used for synthesis because it is a simple process and requires simple reagents like a precursor (zinc nitrate) and a precipitation agent (NaOH). The novelty in the present study lies in the fact that the prepared material can be recycled after 20 cycles of degradation of MB in the presence of a natural light source, namely sunlight [49]. A visible spectrometer is critical in the photodegradation study, as it shows the degradation amount of the original and final reduced MB. The UV spectra of MB show a sharp absorption peak around 664 and 612 nm. This peak at 664 nm is due to the association of the MB monomer and then again towards 612 nm for the MB dimer. In addition, in the UV region, two more peaks at 292 and 245 nm are observed in association with the benzene ring [49].

## 2 Materials

The materials used in this study include zinc nitrate hexahydrate ($Zn(NO_3)_2$), sodium hydroxide (NaOH), silica gel 60–120, MB ($C_{16}H_{18}ClN_3S$), and deionized water. Zinc nitrate and sodium hydroxide were purchased from HIMEDIA and stored in a desiccator to prevent moisture. They were kept in their solid state whenever they were removed from the desiccator and placed back in it for subsequent uses. MB was purchased from SD Fine Laboratory in Mumbai.

## 3 Methods

### 3.1 Preparation of silica-coated ZnO nanoparticles

In the present study, silica-coated ZnO nanoparticles were prepared through a co-precipitation process by using 25 g of silica gel (60–120 mesh) with 100 ml of 1 M zinc nitrate solution and dropwise addition of 1 M NaOH with continuous stirring on a magnetic stirrer at a pH of 10.8. The obtained white precipitate was filtered, washed with deionized water 3–4 times, and then dried in a hot air oven. The resulting powder was calcined at 650°C for 2 h to obtain silica-coated ZnO nanoparticles. The prepared nanoparticles were characterized using X-ray diffraction (XRD), Fourier-transform infrared (FTIR) spectroscopy, and field emission gun–scanning electron microscopy (FEG-SEM).

### 3.2 Preparation of ZnO nanoparticles

ZnO nanoparticles were synthesized using 1 M zinc nitrate hexahydrate solution as the zinc source and 1 M NaOH as a precipitation agent. About 500 ml of 1 M zinc nitrate solution was kept on a magnetic stirrer and 1 M NaOH was added dropwise to maintain a pH of 10.8. The resulting white precipitate was filtered, washed with deionized water 3–4 times, and then dried in a hot air oven. The obtained powder was calcined at 650°C for 2 h to obtain ZnO nanoparticles [1]. The prepared nanoparticles were characterized using XRD, FTIR, and FEG-SEM.

### 3.3 Photodegradation of MB in the presence of bare silica, ZnO, and silica-coated ZnO nanoparticles

The photocatalytic degradation of MB under natural sunlight was studied for bare silica, ZnO, and silica-coated ZnO nanoparticles. The percentage of degradation was observed using Shimadzu's UV-1900i spectrophotometer. For the study, 5 g of bare silica, silica-coated ZnO nanoparticles, and 10 mg of ZnO nanoparticles were taken in a Petri plate and beaker, respectively. The concentration of MB was 10 ppm. A comparative photodegradation analysis was performed for bare silica, ZnO nanoparticles, and Silica@ZnO nanoparticles in the presence of sunlight. MB stock solution (10 ppm, 100 ml) was subjected to sunlight exposure in order to investigate the impact of light on its degradation. The degradation study took place during the period of high light intensity, specifically between 11 a.m. and 3 p.m. The Lux intensity was assessed using a Lutron 1X-103 digital Lux meter, registering an intensity of 6,250 Lux. The used material was also studied, where the MB supernatant was removed and kept under sunlight. Silica and ZnO coated on silica were easily separated and recovered from the reaction due to a larger adsorbent surface area. However, in the case of ZnO nanoparticles, it was not feasible due to their powdery nature and low surface area, which made it difficult to separate them from the reaction.

## 4 Results and discussion

In this study, silica-coated ZnO and ZnO nanoparticles were synthesized using zinc nitrate as a precursor. A modified method involving changes in the temperature and calcination time was used to achieve the synthesis of nanoparticles [50]. The coprecipitation method was employed for the synthesis, wherein zinc nitrate was used as a precursor and the temperature was increased from 200°C to 500°C, resulting in a sharp increase in the XRD pattern. The transmission electron microscopy image showed the hexagonal morphology of the ZnO nanoparticle [51]. The temperature required for the synthesis of ZnO was found to be between 650°C and 700°C, whereas for the synthesis of silica nanoparticles, the temperature range was between 600°C and 1,100°C. For attaching ZnO to silica, annealing at temperatures between 600°C and 700°C was necessary. The effect of temperature was observed to cause changes in the XRD pattern [52]. A higher temperature was required for the synthesis of Silica@ZnO nanoparticles. Stirring time was found to be irrelevant in the synthesis of nanoparticles, as reported in the study of Kanha and Saengkwamsawang [53], and thus, it was eliminated as a variable. Coprecipitation was used as one of the chemical synthesis methods for the nanoparticles, where temperature played a crucial role in the synthesis process [54]. During the synthesis of ZnO on silica, silica was mixed with zinc nitrate and added dropwise with NaOH to form a precipitate. The final pH was adjusted to 11, and the precipitate was filtered through Buckner. The precipitate was washed several times with distilled water to remove the extra salt present in it.

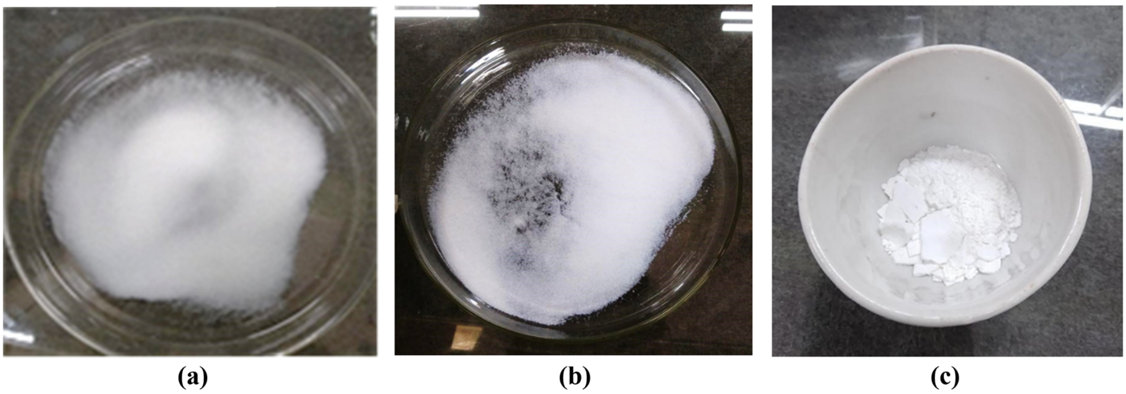
(a) (b) (c)

**Figure 1:** (a) Bare silica without calcination, (b) silica-coated ZnO nanoparticles after calcination, and (c) ZnO nanoparticles after calcination.

**Table 1:** Weight of zinc oxide nanoparticles (ZnO NPs) before and after calcination

| Sample name | Weight before calcination | Weight after calcination |
|---|---|---|
| Silica@ZnO | 34.719 g | 25.306 g |
| Zinc oxide | 2.7500 g | 2.6352 g |

The calcination temperature used for each nanoparticle was 650°C for 3 h. Figure 1a shows the bare silica without calcination, Figure 1b shows the silica-coated ZnO nanoparticles after calcination, and Figure 1c shows the ZnO nanoparticles after calcination.

The weight of Silica@ZnO and ZnO nanoparticles before and after calcination is presented in Table 1. There was a decrease in weight after calcination, attributed to the loss of sodium salt and other impurities. At a high temperature of 650°C, only Silica@ZnO nanoparticles were synthesized. The ZnO deposited on the surface of silica was found to be 80 mg/5 g of Silica@ZnO materials used for the degradation of around 2 l of MB dye. The nanoparticles were stored in an airtight container after calcination and used for further XRD, SEM, FTIR characterization, and photocatalytic dye degradation applications.

## 4.1 Characterization of nanoparticles

### 4.1.1 UV-visible diffuse reflectance spectroscopy (DRS)

The UV-visible DRS analysis of Silica@ZnO nanoparticles is depicted in Figure 2. The observed adsorption band edge, located at 362 nm for silica-coated ZnO, is indicative of the presence of ZnO particles within the sample. Utilizing the relationship $E_{\text{bg}} = 1{,}240/\lambda_{\max}$, where $E_{\text{bg}}$ represents the band gap energy and $\lambda_{\max}$ corresponds to the maximum absorption wavelength, the band gap of ZnO nanoparticles when supported on mesoporous silica was found to be 2.5 eV. In contrast, the band gap energy of pure nano-zinc oxide was found to be 3.50 eV. This significant reduction in band gap energy when ZnO is supported on mesoporous silica implies an enhancement in the photocatalytic performance of ZnO.

### 4.1.2 SEM analysis

The formation of ZnO nanoparticles was confirmed using various characterization techniques. One of the most popular tools for characterizing nanomaterials and nanostructures is the SEM [55]. The signals that result from electron–sample interactions provide details about the sample, such as its chemical composition and surface appearance (texture). In the current study, the silica surface is occupied by ZnO nanoparticles. Figure 3a shows that the ZnO nanoparticles grown on silica surfaces are unevenly distributed. The shape of the nanoparticle is not uniform. Figure 3b shows that the average particle size of Silica@ZnO nanoparticles was 100 nm, spherical and oval.

### 4.1.3 XRD analysis

A non-destructive analytical technique called XRD offers detailed information on the lattice structure of a crystalline

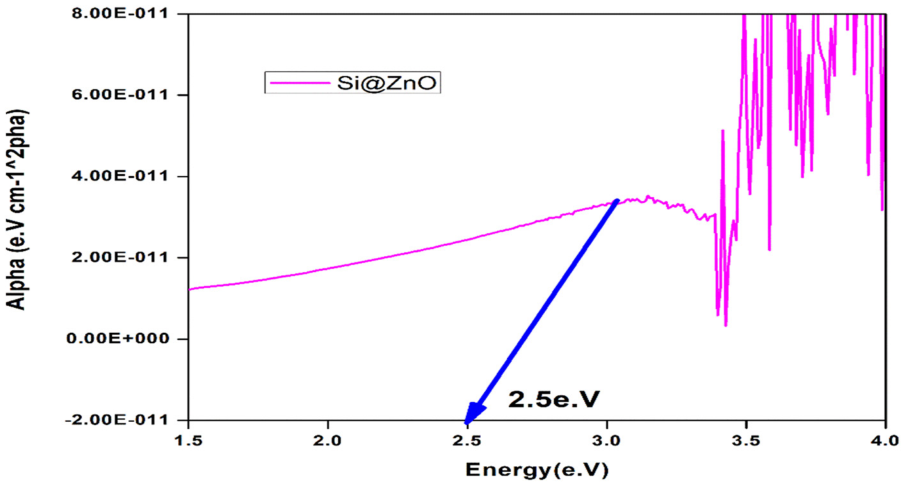

**Figure 2:** Diffuse reflectance UV-vis spectra of Silica@ZnO and the band gap of nanomaterial is 2.5 eV.

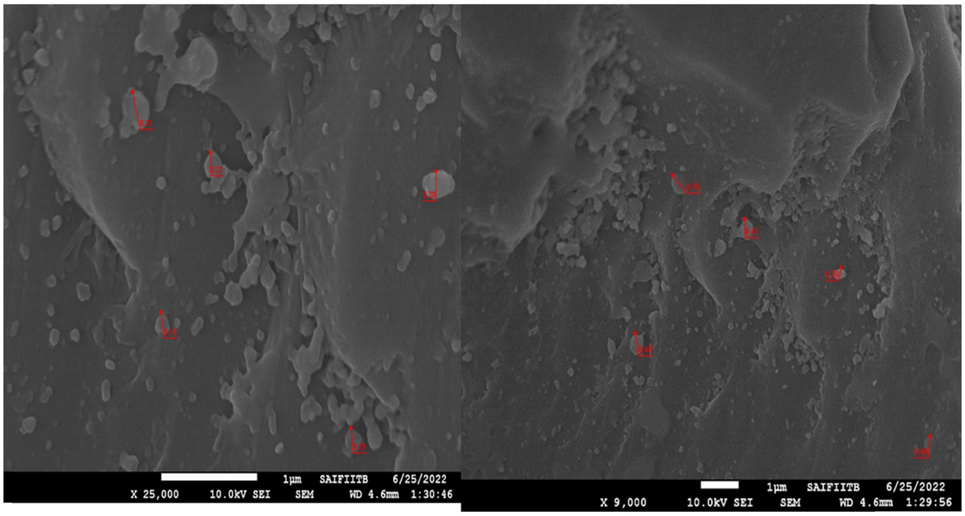

(a) (b)

**Figure 3:** SEM image of Silica@ZnO: (a) at 1 µm scale and (b) at 100 nm scale.

substance, such as unit cell diameters, bond angles, chemical composition, and crystallographic structure of natural and synthetic materials. The quick analytical technique, XRD, is generally used to determine the phase of the crystalline materials and can reveal details like atomic spacing and unit cell size [56]. As silica is an amorphous material, it does not show sharp peaks. Figure 4 shows diffraction peaks at 31.70, 34.42, 36.26, 47.62, 58.73, 62.65, 67.98, 72.54, and 76.90 nm. These peaks agree with the JCPDS Data Card 36-1451, thus, indicating the crystal structure, purity, and crystalline nature of ZnO.

Various techniques were employed to confirm the formation and characteristics of ZnO nanoparticles. SEM was used to analyse the surface appearance and chemical composition of Silica@ZnO nanoparticles. The SEM analysis showed uneven distribution and non-uniform shape of the nanoparticles, with an average size of 100 nm, as revealed in Figure 2a and b. XRD was used to determine the crystalline nature and purity of ZnO. Sharp peaks were observed at 31.70, 34.42, 36.26, 47.62, 58.73, 62.65, 67.98, 72.54, and 76.90 nm, consistent with the JCPDS Data Card 36-1451, indicating the crystal structure of ZnO. Additionally, FTIR spectroscopy was employed to identify functional groups present on the surface of Silica@ZnO nanoparticles.

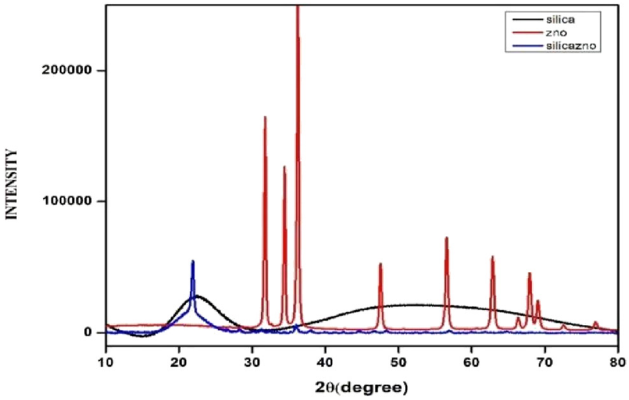

**Figure 4:** XRD pattern of silica, ZnO NPs, and silica-coated ZnO NPs (Silica@ZnO).

### 4.1.4 FTIR analysis

FTIR is a useful technique to analyse the functional groups and chemical bonding of the synthesized nanoparticles. The presence of various functional groups in Silica, Silica@ZnO, and ZnO nanoparticles has been confirmed by FTIR.

The FTIR analysis was conducted on silica, Silica@ZnO, and ZnO nanoparticles to identify the functional groups present. Figure 5 shows FTIR spectra of silica, Silica@ZnO, and ZnO. Silica was found to have 17 clear adsorption bands, indicating the presence of alcohol, aromatic compounds, alkenes, and sulphonates. The analysis showed a peak corresponding to the stretching vibration of O–H stretching vibration at 3,779.9 and 3,374.54 nm, O═C═O stretching vibration at 2,324.43 nm, N═C═S stretching vibration at 2,051.13 nm, and bending vibration of C–H aromatic compounds at 1,981.16 nm. The stretching vibration of C═O was detected at 1,742.14 and 1,684 nm.

Similarly, the FTIR analysis of Silica@ZnO confirmed the presence of alcohol, aromatic compounds, and conjugated aldehydes. However, only eight clear adsorption peaks were identified, indicating that 8 of the 17 functional

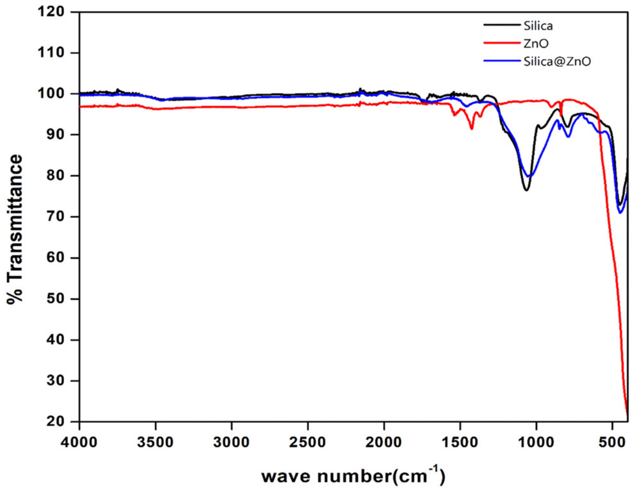

**Figure 5:** FTIR spectra of silica, ZnO NPs, and silica-coated ZnO NPs (Silica@ZnO).

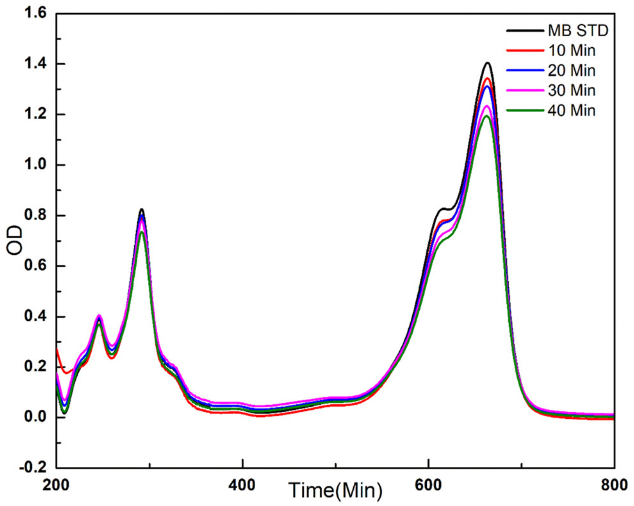

**Figure 6:** Photocatalytic degradation of MB in the absence of a catalyst.

groups of silica were missing due to the presence of ZnO nanoparticles. The stretching vibration of O–H alcohol was found at 3,457.02 nm, the stretching vibration of $N{=}C{=}S$ at 2,051.15 nm, and the bending vibration of the C–H aromatic compound at 1,981.21 nm. The stretching vibration of the conjugated aldehyde was detected at 1,683.94 nm, the bending vibration of $CH_2$ at 1,460.22 nm, the stretching vibration of C–O–C at 1,055.49 nm, and the presence of C–Cl was represented by a peak detected at 790.73 nm.

The absence of some functional groups of silica in Silica@ZnO indicates that the silica was coated with ZnO nanoparticles during the coprecipitation process, where zinc hydroxide accommodates the pores present on the silica and then gets converted into ZnO nanoparticles during the calcination process.

## 5 Photocatalytic activity and recovery of the catalyst

Our aim of the study is the photocatalytic degradation of MB and recovery of the catalyst in the presence of sunlight. For that, MB was degraded in the presence and absence of the catalyst.

A photochemical investigation was conducted on a 10 parts per million (ppm) MB solution to examine its natural degradation under sunlight, without the introduction of any external catalyst. The solution was exposed to sunlight for 40 min, and the results, as illustrated in Figure 6, demonstrated only minimal alterations. These observations strongly suggest that MB, when subjected to sunlight in the absence of a catalyst, does not exhibit substantial degradation

To investigate the photocatalytic activity and the recovery of catalysts, a 100 ml stock solution of MB (10 ppm) was mixed with 5 g of silica, 5 g of Silica@ZnO, and 10 mg of ZnO. The amount of ZnO used is approximately equivalent to ZnO deposited on 5 g of silica-coated ZnO nanoparticles. The mixture was then exposed to sunlight, and the initial concentration of MB was measured to be over 1.5 OD using a UV-Vis spectrophotometer before adding silica, Silica@ZnO, and ZnO. The degradation of MB was monitored by measuring the OD of the samples at 10 min intervals.

The results showed that ZnO nanoparticles had low photocatalytic activity and no recovery due to the aggregation of the nanoparticles. Figure 7 shows the degradation

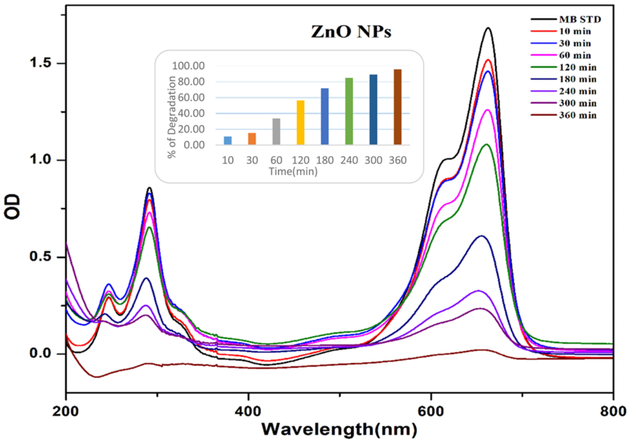

**Figure 7:** Photocatalytic degradation of MB on ZnO NPs. Inset: Percentage of degradation of MB by using ZnO NPs.

of the MB dye on ZnO nanoparticles. It took 120 min for half degradation and 360 min for complete degradation. Furthermore, ZnO nanoparticles could not be reused after the first cycle.

Compared to ZnO, silica has a larger surface area that enables effective adsorption and photodegradation of MB. Simultaneous adsorption and photocatalysis occur, and after 10 min of sunlight exposure, more than 70% of the dye degrades. Complete degradation is achieved in only 40 min, which is faster than the degradation observed in the presence of ZnO. Figure 7 shows the degradation of the MB dye on the first cycle of ZnO nanoparticles.

MB initially adsorbs onto the pores of silica, resulting in blue colouration. However, photocatalysis subsequently takes place, converting the blue silica to white silica in the presence of sunlight. Figure 8a shows the colour changes of Silica@ZnO after one cycle, Figure 8b shows the colour changes of dried silica after 10 min, Figure 8c shows the colour change from dark blue to light blue after 30 min, and Figure 8d shows completely white silica, indicating the complete recovery of silica and ready for the next cycle of degradation. Silica requires approximately 1 h to completely dry, and rapid recovery is possible under bright sunlight. The recovered silica can be used for subsequent cycles of MB dye, with some concentration used in each cycle.

Silica exhibits photodegradation of MB for five consecutive cycles as depicted in Figure 9a and b. In the first cycle, the required time for complete degradation is 40 min, and in the fifth cycle, the time increases to 60 min. However, after the fifth cycle, there is no further adsorption of photocatalysts because all the active sites of bare silica are blocked by MB, leading to the loss of its properties. Due to the extensive adsorption of MB, white silica turns blue and cannot return to its original colour. Notably, bare silica shows a significant increase in photocatalytic activity when compared to ZnO.

The efficiency of silica was enhanced by coating it with ZnO, leading to an increase in photocatalyst efficiency. Silica@ZnO demonstrated a higher photocatalytic activity compared to bare silica, and it continued to exhibit activity

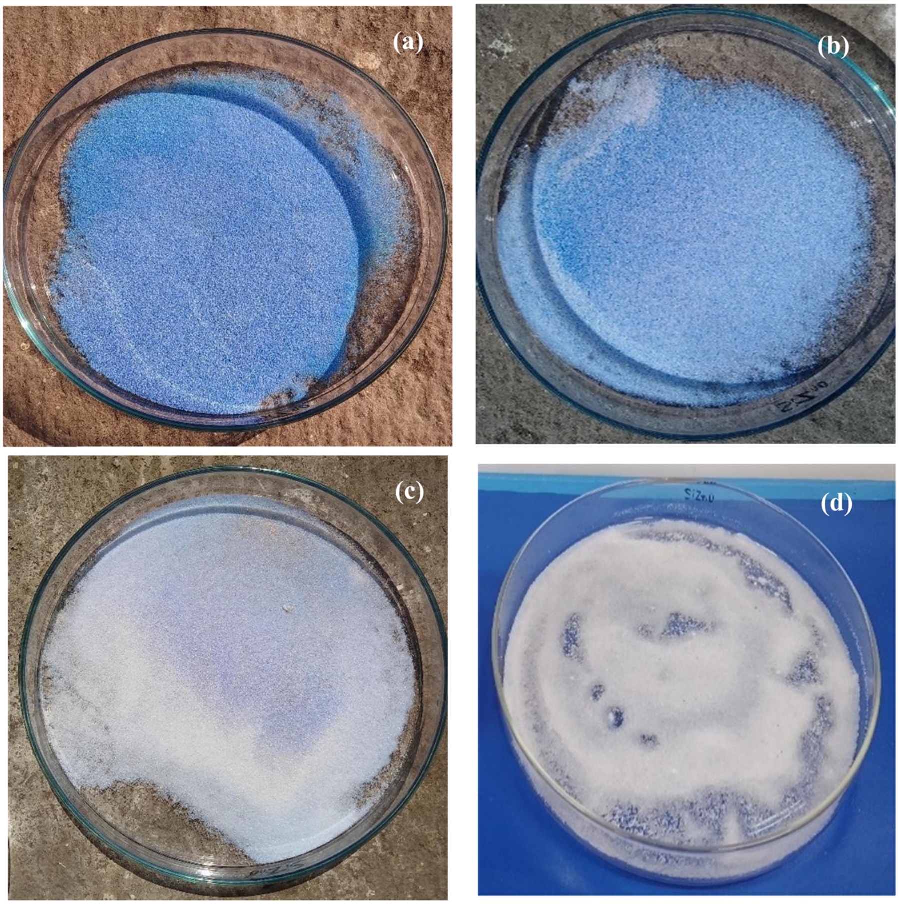

**Figure 8:** (a) Colour changes of Silica@ZnO after one cycle, (b) drying of silica after 10 min, (c) change in colour from dark blue to light blue after 30 min, and (d) complete recovery of Silica@ZnO.

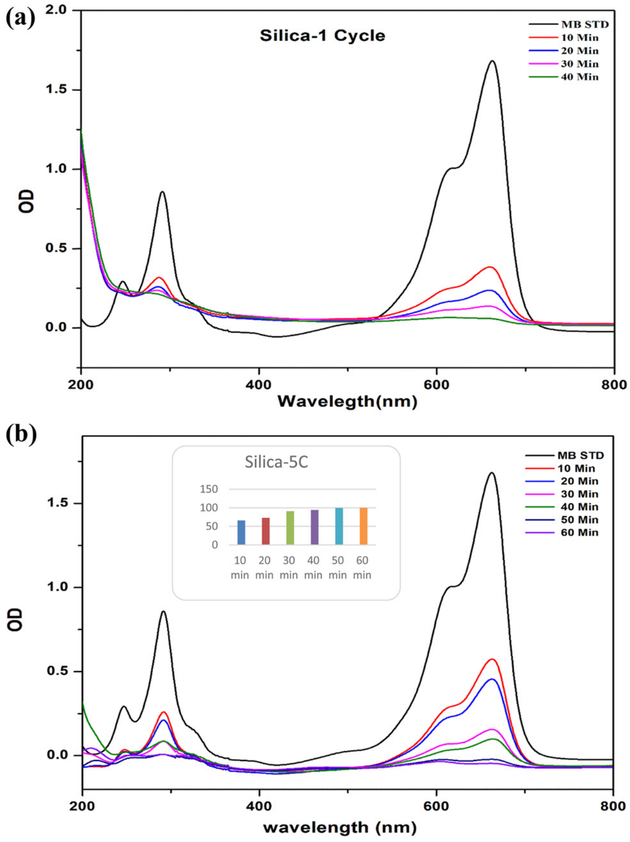

**Figure 9:** Photocatalytic degradation of MB dye on (a) the first cycle of silica and (b) on bare silica during the fifth cycle.

even beyond the fifth cycle, unlike bare silica which became blocked by MB. In the first cycle, the time required for degradation was 40 min, while for the fifth cycle and beyond, it took 60 min. Silica@ZnO was able to undergo photodegradation and regeneration for up to 20 cycles. Although the adsorption capacity of silica was limited to five cycles20 cycles were run on Silica@ZnO.

Figure 10a shows Silica@ZnO at the first cycle of MB, which takes 40 min. After the complete reaction, Silica@ZnO is removed from the reaction and placed in a Petri plate for complete drying. After the colour changes from blue to white, now Silica@ZnO is ready for the next cycle. The same procedure is repeated to check the efficiency of MB dye degradation. Figure 10b shows the degradation of MB degradation on the fifth cycle. The material shows dye degradation efficiency up to 20 cycles.

## 6 Conclusion

The coprecipitation method is an effective way of rapidly synthesizing Silica@ZnO nanoparticles. The synthesized nanoparticles were characterized using XRD, FTIR, SEM, and EDX, and their formation was confirmed by XRD and SEM. FTIR analysis showed that eight functional groups of silica were reduced during the synthesis and coating process. The photocatalytic activity was studied using MB dye, with ZnO nanoparticles used in the first cycle due to the difficulty in collecting them. Silica@ZnO was found to have both adsorption and degradation properties, with the capacity to degrade up to 200 ppm of MB on 5 g of the material. The synthesized Silica@ZnO was able to perform up to 20 cycles of degradation, indicating it is a highly efficient photocatalyst with excellent recovery. The low-cost method of synthesis makes Silica@ZnO a promising option for environmental remediation in industries such as textiles and paper for dye degradation and water purification.

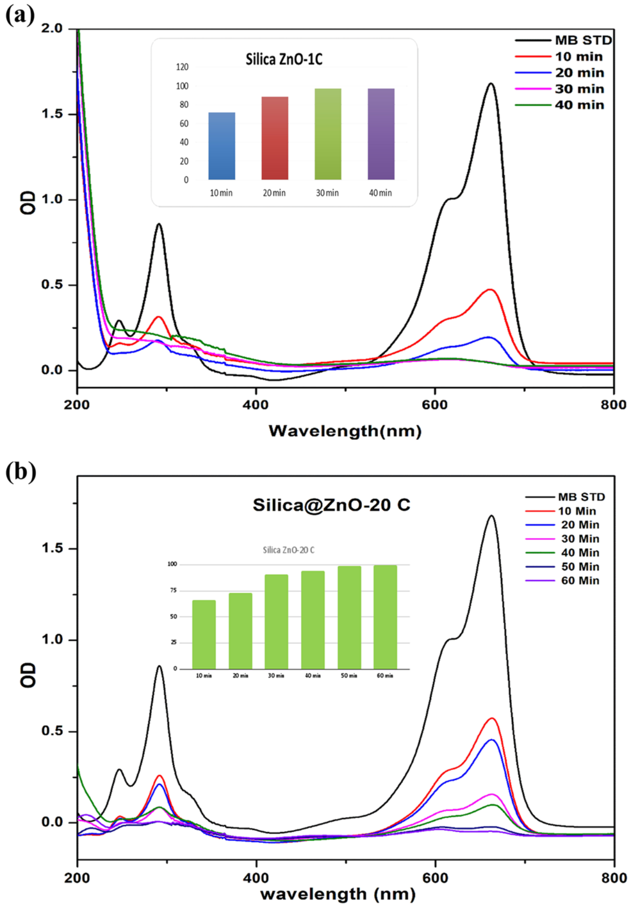

**Figure 10:** (a) Photocatalytic degradation of MB on (a) the first cycle of Silica@ZnO/Silica ZnO and (b) on the fifth cycle of Silica@ZnO.

## 7 Future prospects

In the current study, silica is used as a supporting matrix for the ZnO nanoparticle synthesis but other supportive matrices including natural and synthetic matrices can also exhibit good adsorptive and recyclable properties. The incorporation of metal oxide like ZnO was responsible for increasing the adsorptive and recycling capacity of silica. Instead of ZnO, other metal oxides like $TiO_2$, CuO, nanoparticles, etc., can in the future serve the same function.

**Acknowledgments:** The authors are grateful to the CSIR-UGC (JUNE -359427) for giving JRF a stipend during research work.

**Funding information:** Stipend funding from CSIR-UGC (JUNE -359427) was received.

**Author contributions:** All the authors have equally contributed to the conceptualization, methodology, draft preparation, and data interpretation. The corresponding authors contributed to draft preparation and reviewed the manuscript.

**Conflict of interest:** The authors state no conflict of interest.

**Data availability statement**: All data generated or analysed during this study are included in this published article.

## References

[1] Barnett JR, Miller S, Pearce E. Colour and art: A brief history of pigments. Opt Laser Technol. 2006;38(4–6):445–53. doi: 10.1016/j.optlastec.2005.06.005.

[2] Kant R. Textile dyeing industry an environmental hazard. Nat Sci. 2012;4(1):22–6. doi: 10.4236/ns.2012.41004.

[3] Liu Q. Pollution and treatment of dye waste-water. IOP Conf Ser Earth Environ Sci. 2020;514(5). doi: 10.1088/1755-1315/514/5/052001.

[4] Lellis B, Fávaro-Polonio CZ, Pamphile JA, Polonio JC. Effects of textile dyes on health and the environment and bioremediation potential of living organisms. Biotechnol Res Innov. 2019;3(2):275–90. doi: 10.1016/j.biori.2019.09.001.

[5] Hassan MM, Carr CM. A critical review on recent advancements of the removal of reactive dyes from dyehouse effluent by ion-exchange adsorbents. Chemosphere. Elsevier Ltd; 2018 Oct:209:201–19. doi: 10.1016/j.chemosphere.2018.06.043.

[6] Syamani FA. Cellulose-based membrane for adsorption of dye in batik industry wastewater. Int J Hydrol. 2020;4(6):281–3. doi: 10.15406/ijh.2020.04.00255.

[7] Atalay S, Ersöz G. Advanced oxidation processes for removal of dyes from aqueous media. In: Green chemistry for dyes removal from waste water: Research trends and applications. Valentina: Wiley; 2015. p. 83–117.

[8] Samarghandi MR, Dargahi A, Shabanloo A, Nasab HZ, Vaziri Y, Ansari A. Electrochemical degradation of methylene blue dye using a graphite doped PbO2 anode: Optimization of operational parameters, degradation pathway and improving the biodegradability of textile wastewater. Arab J Chem. 2020 Aug;13(8):6847–64. doi: 10.1016/j.arabjc.2020.06.038.

[9] Gadekar MR, Ahammed MM. Coagulation/flocculation process for dye removal using water treatment residuals: modeling through artificial neural networks. Desalin Water Treat. 2016 Nov;57(55):26392–400. doi: 10.1080/19443994.2016.1165150.

[10] Ruan W, Hu J, Qi J, Hou Y, Zhou C, Wei X. Removal of dyes from wastewater by nanomaterials: A review. Adv Mater Lett. 2019;10(1):9–20. doi: 10.5185/amlett.2019.2148.

[11] Ankamwar BG, Kamble VB, Annsi JI, Sarma LS, Mahajan CM. Solar photocatalytic degradation of methylene blue by ZnO nanoparticles. J Nanosci Nanotechnol. 2017;17(2):1185–92. doi: 10.1166/jnn.2017.12579.

[12] Irani M, Mohammadi T, Mohebbi S. Photocatalytic degradation of methylene blue with ZnO nanoparticles; a joint experimental and theoretical study. J Mex Chem Soc. 2016;60(4):218–25. doi: 10.29356/jmcs.v60i4.115.

[13] Ghoniem MG, Talab SA, Modwi AK, Taha KK. Exploration of Methylene Blue Degradation over ZnO Nanorods Mechanism using Scavenging Reagents. Orient J Chem. 2021 Jun;37(3):609–18. doi: 10.13005/ojc/370313.

[14] El-Shazly AN, Rashad MM, Abdel-Aal EA, Ibrahim IA, El-Shahat MF, Shalan AE. Nanostructured ZnO photocatalysts prepared via surfactant-assisted Co-Precipitation method achieving enhanced photocatalytic activity for the degradation of methylene blue dyes. J Environ Chem Eng. 2016;4(3):3177–84. doi: 10.1016/j.jece.2016.06.018.

[15] Kolodziejczak-Radzimska A, Jesionowski T. Zinc oxide-from synthesis to application: A review. Materials (Basel). 2014;7(4):2833–81. doi: 10.3390/ma7042833.

[16] Vanaja M, Paulkumar K, Baburaja M, Rajeshkumar S, Gnanajobitha G, Malarkodi C, et al. Degradation of methylene blue using biologically synthesized silver nanoparticles. Bioinorg Chem Appl. 2014;2014:742346. doi: 10.1155/2014/742346.

[17] Dabhane H, Chatur S, Jadhav G, Tambade P, Medhane V. Phytogenic synthesis of gold nanoparticles and applications for removal of methylene blue dye: A review. Environ Chem Ecotoxicol. 2021;3:160–71. doi: 10.1016/j.enceco.2021.04.002.

[18] Kora AJ, Rastogi L. Catalytic degradation of anthropogenic dye pollutants using palladium nanoparticles synthesized by gum olibanum, a glucuronoarabinogalactan biopolymer. Ind Crops Prod. 2016 Mar;81:1–10. doi: 10.1016/j.indcrop.2015.11.055.

[19] Jassim HA, Khadhim A, Al-Amiery AA. Photo catalytic degradation of methylene blue by using CuO nanoparticles. Int J Comput Appl Sci. 2016 Dec;1(3):1–4. doi: 10.24842/1611/0011.

[20] Jayakumar G, Albert Irudayaraj A, Dhayal Raj A. Photocatalytic degradation of methylene blue by nickel oxide nanoparticles. Mater Today Proc. 2017 Jan. 4(11):11690–5. doi: 10.1016/j.matpr.2017.09.083.

[21] Sackey J, Bashir AKH, Ameh AE, Nkosi M, Kaonga C, Maaza M. Date pits extracts assisted synthesis of magnesium oxides nanoparticles and its application towards the photocatalytic degradation of methylene blue. J King Saud Univ – Sci. 2020 Sep;32(6):2767–76. doi: 10.1016/j.jksus.2020.06.013.

[22] Vasiljevic ZZ, Dojcinovic MP, Vujancevic JD, Jankovic-Castvan I, Ognjanovic M, Tadic NB. Photocatalytic degradation of methylene

blue under natural sunlight using iron titanate nanoparticles prepared by a modified sol-gel method: Methylene blue degradation with Fe2TiO5. R Soc Open Sci. 2020;7(9). doi: 10.1098/rsos.200708.

[23] Lazar MA, Varghese S, Nair SS. Photocatalytic water treatment by titanium dioxide: Recent updates. Catalysts. 2012 Dec;2(4):572–601. doi: 10.3390/CATAL2040572.

[24] Petrovičová B, Dahrouch Z, Triolo C, Pantò F, Malara A, Patanè S, et al. Photocatalytic degradation of methylene blue dye by electrospun binary and ternary zinc and titanium oxide nanofibers. Appl Sci. 2021;11(20):9720. doi: 10.3390/app11209720.

[25] Eddy DR, Noviyanti AR, Solihudin S, Ishmayana S, Tjokronegoro R. Rice husk for photocatalytic composite material fabrication. Visible-Light Photocatalysis Carbon-Based Materials. London, UK: IntechOpen; 2018. p. 0–9. doi: 10.5772/intechopen.72704.

[26] Arami M, Limaee NY, Mahmoodi NM, Tabrizi NS. Removal of dyes from colored textile wastewater by orange peel adsorbent: Equilibrium and kinetic studies. J Colloid Interface Sci. 2005 Aug;288(2):371–6. doi: 10.1016/j.jcis.2005.03.020.

[27] Bose S, Ghosh A, Das A, Rahaman M. Development of mango peel derived activated carbon-nickel nanocomposite as an adsorbent towards removal of heavy metal and organic dye removal from aqueous solution. ChemistrySelect. 2020 Nov;5(44):14168–76. doi: 10.1002/slct.202003606.

[28] Józwiak T, Filipkowska U, Bugajska P, Kalkowski T. The use of coconut shells for the removal of dyes from aqueous solutions. J Ecol Eng. 2018;19(4):129–35. doi: 10.12911/22998993/89672.

[29] Qamar SA, Ashiq M, Jahangeer M, Riasat A, Bilal M. Chitosan-based hybrid materials as adsorbents for textile dyes–A review. Case Stud Chem Environ Eng. 2020 Sep;2:100021. doi: 10.1016/j.cscee.2020.100021.

[30] Lafi R, ben Fradj A, Hafiane A, Hameed BH. Coffee waste as potential adsorbent for the removal of basic dyes from aqueous solution. Korean J Chem Eng. 2014 Nov;31(12):2198–206. doi: 10.1007/s11814-014-0171-7.

[31] Akter M, Rahman FBA, Abedin MZ, Kabir SMF. Adsorption characteristics of banana peel in the removal of dyes from textile effluent. Textiles. 2021 Sep;1(2):361–75. doi: 10.3390/textiles1020018.

[32] Yu ZH, Zhai SR, Guo H, lv TM, Song Y, Zhang F, et al. Removal of methylene blue over low-cost mesoporous silica nanoparticles prepared with naturally occurring diatomite. J Sol-Gel Sci Technol. 2018;88(3):541–50. doi: 10.1007/s10971-018-4859-8.

[33] López-Rodríguez D, Micó-Vicent B, Jordán-Núñez J, Bonet-Aracil M, Bou-Belda E. Uses of nanoclays and adsorbents for dye recovery: A textile industry review. Appl Sci (Switzerland). 2021 Dec;11(23):11422. doi: 10.3390/app112311422. MDPI.

[34] Bello OS, Bello IA, Adegoke KA. Adsorption of dyes using different types of sand: A review. S Afr J Chem. 2013, Accessed: 28 Jun 2022;66:117–29, http://journals.sabinet.co.za/sajchem/.

[35] Bankole AA, Poulose V, Ramachandran T, Hamed F, Thiemann T. Comparative study of the selective sorption of organic dyes on inorganic materials—A cost-effective method for waste treatment in educational and small research laboratories. Separations. 2022 Jun;9(6):144. doi: 10.3390/separations9060144.

[36] Hussain MJIAAM. "2078-9337-1-CE.pdf." J Chem Soc PAK. 1993 Nov;15:7–10. Pakistan.

[37] Narayan R, Nayak UY, Raichur AM, Garg S. Mesoporous silica nanoparticles: A comprehensive review on synthesis and recent advances. Pharmaceutics. 2018 Sep;10(3):1118. MDPI AG doi: 10.3390/pharmaceutics10030118.

[38] Janani R, Gurunathan B, Sivakumar K, Varjani S, Ngo HH, Gnansounou E. Advancements in heavy metals removal from effluents employing nano-adsorbents: Way towards cleaner production. Environ Res. 2021 Aug;203:111815. doi: 10.1016/j.envres.2021.111815. p. 2022.

[39] Dhiman M, Singh B, Polshettiwar V. Silica-supported nanoparticles as heterogeneous catalysts. Nanoparticles in Catalysis. Wiley. 2021; p. 215–38. doi: 10.1002/9783527821761.ch10.

[40] Azmina MS, Nor RM, Rafaie HA, Razak NSA, Sani SFA, Osman Z. Enhanced photocatalytic activity of ZnO nanoparticles grown on porous silica microparticles. Appl Nanosci. 2017;7(8):885–92. doi: 10.1007/s13204-017-0626-3.

[41] Dagher S, Soliman A, Ziout A, Tit N, Hilal-Alnaqbi A, Khashan S, et al. Photocatalytic removal of methylene blue using titania- and silica-coated magnetic nanoparticles. Mater Res Express. 2018 Jun;5(6):065518. doi: 10.1088/2053-1591/AACAD4.

[42] Prodjosantoso AK, Kamilia S, Utomo MP, Budiasih KS. Silica supported copper-nickel oxide catalyst for photodegradation of methylene blue. Asian J Chem. 2019;31(12):2891–6. doi: 10.14233/AJCHEM.2019.22284.

[43] Quiton KGN, Lu MC, Huang YH. Synergistic degradation of Methylene Blue by novel Fe-Co bimetallic catalyst supported on waste silica in the photo-Fenton-like system. Sustain Environ Res. 2022 Dec;32(1):1–18. doi: 10.1186/S42834-022-00127-W/FIGURES/12.

[44] Shamspur T, Mostafavi A, Ziaadini F, Fathirad F. Photocatalytic degradation of methylene blue from aqueous solution using fe3o4@sio2@ceo2 core-shell magnetic nanostructure as an effective catalyst. Adv Environ Technol. 2019;5(2):127–32. doi: 10.22104/aet.2020.4137.1204.

[45] Istiqomah NI, Muzakki AT, Nofrianti A, Suharyadi E, Kato T, Iwata S. The effect of silica on photocatalytic degradation of methylene blue using silica-coated in ferrite nanoparticles. Key Eng Mater. 2020;855:268–73. doi: 10.4028/www.scientific.net/KEM.855.268.

[46] Beagan AM. Investigating methylene blue removal from aqueous solution by cysteine-functionalized mesoporous silica. J Chem. 2021;2021:1–12. doi: 10.1155/2021/8839864.

[47] Almethen AA, Alotaibi KM, Alhumud HS, Alswieleh AM. Highly efficient and rapid removal of methylene blue from aqueous solution using folic acid-conjugated dendritic mesoporous silica nanoparticles. Processes. 2022;10(4):705. doi: 10.3390/pr10040705.

[48] Parida D, Salmeia KA, Sadeghpour A, Zhao S, Maurya AK, Assaf KI, et al. Template-free synthesis of hybrid silica nanoparticle with functionalized mesostructure for efficient methylene blue removal. Mater Des. 2021;201:109494. doi: 10.1016/j.matdes.2021.109494.

[49] Khan I, Saeed K, Zekker I, Zhang B, Hendi AH, Ahmad A, et al. Review on methylene blue: Its properties, uses, toxicity and photodegradation. Water (Switzerland). 2022;14(2):242. doi: 10.3390/w14020242.

[50] Devi PG, Velu AS. Synthesis, structural and optical properties of pure ZnO and Co-doped ZnO nanoparticles prepared by the co-precipitation method. J Theor Appl Phys. 2016;10(3):233–40. doi: 10.1007/s40094-016-0221-0.

[51] Farahmandjou M, Jurablu S. Co-precipitation Synthesis of Zinc Oxide (ZnO) Nanoparticles by Zinc Nitrate Precursor. Int J Bio-Inorg Hybrid Nanomater. 2014;3(3):179–84, http://ijbihn.iauvaramin.ac.ir/article_640348.html.

[52] Bensmaine S, Benyoucef B. Effect of the temperature on ZnO thin films deposited by r.f. magnetron. Phys Procedia. 2014;55:144–9. doi: 10.1016/j.phpro.2014.07.021.

[53] Kanha P, Saengkwamsawang P. Effect of stirring time on the morphology and crystalline features of $MnO_2$ nanoparticles synthesized by co-precipitation method. Inorg Nano-Metal Chem. 2017;47(8):1129–33. doi: 10.1080/24701556.2017.1284100.

[54] Ahamed AJ, Kumar PV. Synthesis and characterization of ZnO nanoparticles by co-precipitation method at room temperature. J Chem Pharm Res. 2016;8(5):624–8. Available online www.jocpr.com.

[55] El-Nahhal IM, Salem JK, Kuhn S, Hammad T, Hempelmann R, Al Bhaisi S. Synthesis and characterization of silica-coated and functionalized silica-coated zinc oxide nanomaterials. Powder Technol. 2016;287:439–46. doi: 10.1016/j.powtec.2015.09.042.

[56] Sahu S, Samanta PK. Peak profile analysis of X-ray diffraction pattern of zinc oxide nanostructure. J Nano-Electron Phys. 2021;13(5):1–4. doi: 10.21272/jnep.13(5).05001.